

Detection of Monkeypox Among Different Pox Diseases with Different Pre-Trained Deep Learning Models

Muhammed ÇELİK^{1*}, Özkan İNİK¹

Highlights:

- Efficiencies of state-of-the-art CNN models on pox diseases were examined.
- These efficiencies were tested on the original and augmented data sets.
- The model with the highest accuracy was obtained for both datasets.

Keywords:

- Monkeypox
- VggNet
- GoogLeNet
- MobileNet
- EfficientNet

ABSTRACT:

Monkeypox is a viral disease that has recently rapidly spread. Experts have trouble diagnosing the disease because it is similar to other smallpox diseases. For this reason, researchers are working on artificial intelligence-based computer vision systems for the diagnosis of monkeypox to make it easier for experts, but a professional dataset has not yet been created. Instead, studies have been carried out on datasets obtained by collecting informal images from the Internet. The accuracy of state-of-the-art deep learning models on these datasets is unknown. Therefore, in this study, monkeypox disease was detected in cowpox, smallpox, and chickenpox diseases using the pre-trained deep learning models VGG-19, VGG-16, MobileNet V2, GoogLeNet, and EfficientNet-B0. In experimental studies on the original and augmented datasets, MobileNet V2 achieved the highest classification accuracy of 99.25% on the augmented dataset. In contrast, the VGG-19 model achieved the highest classification accuracy with 78.82% of the original data. Considering these results, the shallow model yielded better results for the datasets with fewer images. When the amount of data increased, the success of deep networks was better because the weights of the deep models were updated at the desired level.

¹ Muhammed ÇELİK ([Orcid ID: 0000-0001-6909-7830](https://orcid.org/0000-0001-6909-7830)), Özkan İNİK ([Orcid ID: 0000-0003-4728-8438](https://orcid.org/0000-0003-4728-8438)), Tokat Gaziosmanpaşa University, Faculty of Engineering and Architecture, Department of Computer Engineering, Tokat, Türkiye

*Corresponding Author: Muhammed ÇELİK, e-mail: muhammed.celik@gop.edu.tr

INTRODUCTION

Monkeypox is a viral disease transmitted from animals to humans that has clinical symptoms previously seen in smallpox patients but is less severe. Monkeypox first occurred in the tropical rainforest regions of Central and Western Africa, where it has spread to other regions. The disease is transmitted by close contact with an infected person or animal, or by contact with infected materials. The typical clinical symptoms of monkeypox include fever, rash, and swollen lymph nodes, which can lead to various complications. These symptoms usually last 2-4 weeks but can be very severe. Recent case fatality rates range from 3% to 6% (WHO, 2022). Vaccines previously developed for smallpox are used to prevent and protect against the disease, and vaccines are also being developed specifically for monkeypox. This disease is called monkeypox because it emerged among macaque monkeys in an animal facility in Denmark in 1958 while they were not the host of the virus (Memariani and Memariani, 2022). Monkeypox was first observed in humans in 1970 in the Democratic Republic of the Congo (Parker and Buller, 2013). In 2003, an outbreak was caused by animal shipment from Ghana to the United States. Currently, human monkeypox is observed in 10 African countries and four countries outside Africa (Bunge et al., 2022). According to CDC data, as of October 2022, a total of 28302 cases were seen in the United States and only 6 of them resulted in death. The global number of cases was recorded as 76806 (CDC, 2022).

Similar to any other disease, early diagnosis is important for monkeypox. Early diagnosis is vital for preventing this disease and reducing the risk of contamination. However, a wide range of diseases can occur on the skin. These include other smallpox diseases, cancers, and other lesions. For this reason, it can be very difficult to diagnose monkeypox visually. For this, experts resort to methods such as pathology, where they can obtain definitive results, but this causes both a loss of time for early diagnosis of the disease and high costs in terms of cost. Given the lack of adequate laboratory facilities in most countries, diagnosis, isolation, and treatment are delayed, which can lead to further infection and death. For these reasons, researchers have developed various methods for the AI-assisted diagnosis of skin diseases (Alenezi et al., 2023; Bhatt et al., 2022; Elashiri et al., 2022; Monisha et al., 2018; Qian et al., 2022; Wei et al., 2022; Xin et al., 2022).

Today, machine learning (ML) and deep learning (DL) methods are widely used for early diagnosis of many diseases. For this purpose, various imaging modalities and datasets obtained from medical data are used. In particular, deep learning methods are very successful in classification problems (Bayat and Işık, 2022; O. Inik et al., 2019; Ö. Inik and Turan, 2018) and shorten the early diagnosis process by inferring from images in the diagnosis of multi-class diseases, such as brain tumors. Deep learning methods are widely used in many medical classification problems, such as the classification of dermatological diseases (Zhou et al., 2022), cardiovascular diseases (Li et al., 2023), Alzheimer's disease (Hu et al., 2022), Parkinson's disease (Rezaee et al., 2022), chest diseases (Ibrahim et al., 2021), colon cancer and diseases (Pacal et al., 2020; Pacal and Karaboga, 2021) breast cancer (İ. Pacal, 2022), and brain tumors (Jia and Chen, 2020). Likewise, studies have been conducted on the classification and diagnosis of the above-mentioned diseases using ML methods (Aljaddouh and Malathi, 2022; Bhattacharjee et al., 2022; Ferreira et al., 2022; Shinde et al., 2022; Swathy and Saruladha, 2022; Vankdothu and Hameed, 2022; Vuidel et al., 2022). In addition, there are also hybrid studies in the literature where ML and DL methods are used together to achieve high success in the diagnosis of diseases (Alenezi et al., 2023; Nguyen et al., 2022; Rezaee et al., 2022; Talukder et al., 2022).

As with the diagnosis of other diseases, there are several studies in the literature on the diagnosis of monkeypox. These studies were conducted using datasets created by the authors. (Ali et al., 2022) conducted a study to classify skin lesions using pre-trained CNN models on a self-created dataset, including measles, monkeypox, and chickenpox. ResNet50, VGG16 and InceptionV3 models were used as pre-trained CNN models in the study. As a result of the experimental studies, the highest classification accuracy of 82.96% was achieved. (Islam et al., 2022) created a web-scrabbing-based dataset to pioneer studies in this field owing to the scarcity of skin images of monkeypox disease and conducted a study on this dataset. The dataset includes 6 classes: monkeypox, cowpox, chickenpox, smallpox, measles and healthy. In the study, 7 different pre-trained CNN models were used. As a result of the experimental studies, the ShuffleNet-V2 model reached the highest rate with 79%. (Ahsan et al., 2022) created their own dataset, as in previous studies, and trained it on a modified VGG16 network. As a result of the training, they achieved an 83% classification accuracy. (Muñoz-Saavedra et al., 2022) used a dataset of 100 images for automatic diagnosis of monkeypox using 5 individual CNN models and 3 different ensemble models. As a result of the experimental studies, the Ensemble 3 (ResNet50 + EfficientNet-B0 + MobileNet-V2) model achieved a 98% classification accuracy.

In this study, the pre-trained VGG-19, VGG-16, MobileNet V2, GoogLeNet, and EfficientNet-B0 CNN models were used for monkeypox diagnosis. The experiments were performed on both the augmented and original datasets. As a result of the experiments, MobileNet V2 achieved the highest classification accuracy for the augmented data, and VGG-19 for the original data.

The rest of the paper is organised as: Section 2 presents the material and method. In section 3, experimental results that include performance criteria and comparison results. Section 4 is conclusion that explains the results.

MATERIALS AND METHODS

Dataset

This study uses the monkeypox 2022 remastered (Kaggle, 2022) dataset, which was created for the diagnosis of monkeypox and contains images of cowpox, chickenpox, measles, and smallpox, in addition to monkeypox.



Figure 1. Example images of skin lesions from dataset

The dataset contains data filed in two different formats: `preprocessed_original_images` and `augmented_images`. `preprocessed_original_images` file contains the original unprocessed images, whereas `augmented_images` file contains the augmented data. `augmented_images` file contains 8722 chickenpox, 2646 cowpox, 2450 healthy, 2303 measles, 7840 monkeypox and 17542 smallpox images. `preprocessed_original_images` file contains 178 chickenpox, 54 cowpox, 50 healthy, 47 measles, 160 monkeypox, and 358 smallpox images. Both augmented data and raw original data were used in this study. Figure 1 shows a few examples of this dataset.

The sizes of the images in `preprocessed_original_images` file are different from each other; therefore, they are not suitable for training. For this reason, the images in this file were processed and converted to $224 \times 224 \times 3$ pixels to make them suitable for the models to be applied. The images in both files were used during the training and validation phases. The training and validation data were split into 80% and 20%, respectively. The details regarding the number of images are presented in Table 1.

Table 1. Distribution of image classes

| Class | Original Images | Train (80%) | Validation (20%) | Augmented Images | Train (80%) | Validation (20%) |
|--------------|-----------------|-------------|------------------|------------------|-------------|------------------|
| Chickenpox | 178 | 142 | 36 | 8722 | 6978 | 1744 |
| Cowpox | 54 | 43 | 11 | 2646 | 2116 | 530 |
| Measles | 47 | 37 | 10 | 2303 | 1843 | 460 |
| Monkeypox | 160 | 128 | 32 | 7840 | 6272 | 1568 |
| Smallpox | 358 | 286 | 72 | 17542 | 14034 | 3508 |
| Healthy | 50 | 40 | 10 | 2450 | 1960 | 490 |
| Total | 847 | 676 | 171 | 41503 | 33203 | 8300 |

Pre-Trained CNN Models

CNN models are generally deep neural networks used for image classification. In addition, they can perform classifications by inferring audio and numerical data. Many CNN architectures have been proposed in the literature. In this study, five of the most widely used CNN architectures were selected. These architectures were VGG-19, VGG-16, MobileNet V2, GoogLeNet, and EfficientNet-B0. GoogLeNet is a CNN network with 22 layers deep Inception architecture. The input layer accepts a $224 \times 224 \times 3$ image. Because it was trained on the ImageNet dataset, it has an output layer with 1000 classes. MobileNet V2 is a convolutional neural network architecture designed to perform well on mobile devices with 53 layer depth. The architecture has 32 convolution layers, followed by 19 residual bottleneck layers. It has $224 \times 224 \times 3$ input and 1000 class output layers. EfficientNet-B0 is a CNN network designed for image classification with a depth of 82 layers and trained with millions of data. The main advantage of this architecture over other architectures is that it uses a set of constant scaling coefficients to scale all dimensions of depth, width, and resolution equally. By default, EfficientNet-B0 has $224 \times 224 \times 3$ input layers and 1000 class output layers. VGG-16 and VGG-19 were named based on their layer depths. VGG-16 and VGG-19 have layer depths of 16 and 19, respectively. The most important features of these two architectures are their low filter and pooling sizes. They have an input layer of $224 \times 224 \times 3$ and an output layer of 1000 classes. Table 2 lists the characteristics of these architectures.

Table 2. Features of the pretrained CNN models

| Model | Depth | Parameters (Millions) | Image Input Size |
|-----------------|-------|-----------------------|---------------------------|
| VGG-16 | 16 | 138 | $224 \times 224 \times 3$ |
| VGG-19 | 19 | 144 | $224 \times 224 \times 3$ |
| EfficientNet-B0 | 82 | 5.3 | $224 \times 224 \times 3$ |
| MobileNet V2 | 53 | 3.5 | $224 \times 224 \times 3$ |
| GoogLeNet | 22 | 7 | $224 \times 224 \times 3$ |

Method

There are many pretrained CNN models in the literature that are used to classify images for various reasons. In this study, pretrained models that have 224x224 input size were chosen to classify skin lesion images. These models were VGG-16, VGG-19 (Simonyan and Zisserman, 2014), EfficientNet-B0 (Tan and Le, 2019), GoogLeNet (Krizhevsky, 2014), and MobileNet V2 (Sandler et al., 2018). These models have output layers with 1000 classes. Therefore, before the training phase the output layers of the models were replaced with the output layers with 6 classes.

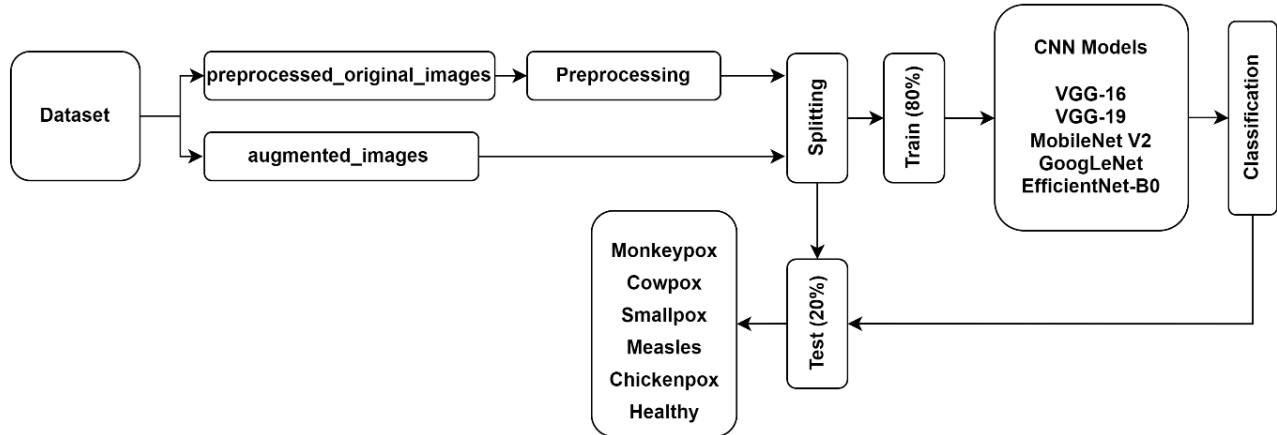


Figure 2. Schematic presentation of the method

Figure 2 clearly illustrates the methodology applied. The dataset is described in detail in the previous section. The images in the augmented_images folder are 224x224x3 in size to be applied to the models. However, because the images in the preprocessed_original_images folder were of different sizes, they were preprocessed and resized to 224x224x3 pixels before being fed to the models. The processed images were divided into training (80%) and validation (20%). The models were semi-trained separately for the original and augmented datasets. Five different CNN models were used for training. Information about these CNN models were given in the previous section. Each model was trained for two separate processed data sets and classification results were obtained. To evaluate the training performance of the models, they were validated with validation data, and the results are presented in detail in the next section.

RESULTS AND DISCUSSION

In this section, results are presented. In the experimental studies, the deep learning library was implemented using MATLAB 2022b software. The computer's technical specifications for use in the experiments are as follows: Intel(R) Core (TM) i5-8400 CPU @ 2.80GHz (6 CPUs), 2.8GHz, 16 GB RAM, and GPU NVIDIA GeForce GTX 1080 Ti with 11 GB memory.

Performance Criteria

The model performances were evaluated using the validation results with the help of certain performance criteria. Accuracy, precision, recall, F1-score and AUC values were used as performance criteria. These values were obtained using confusion matrices. The formulas for the employed metrics are shown in equations (1) – (5).

$$Accuracy = \frac{TP + TN}{TP + TN + FP + FN} \times 100 \quad (1)$$

$$Precision = \frac{TP}{TP + FP} \quad (2)$$

$$Recall = \frac{TP}{TP + FN} \tag{3}$$

$$F1 - score = \frac{2TP}{2TP + FP + FN} \tag{4}$$

$$AUC = \frac{\sum r_i(x_p) - x_p(x_p + 1)/2}{x_p + x_n} \tag{5}$$

where, TP is True Positive, TN is True Negative, FP is False Positive and FN is False Negative. x_p and x_n represent positive and negative samples of data respectively, r_i represents the rating of the i th positive sample. The results are shown in Tables 3 - 4.

Comparison Results

This section presents the results obtained from experimental studies. The performance metrics described in the previous section were used to compare the model performance. To do this, confusion matrices obtained from the validation phases after the training phases of the models were used. The TP , TN , FP , and FN values obtained for each class using confusion matrices were used to calculate the performance metrics. The confusion matrices obtained from the original and augmented data are shown in Figures 3, 4, 5 and 6 respectively.

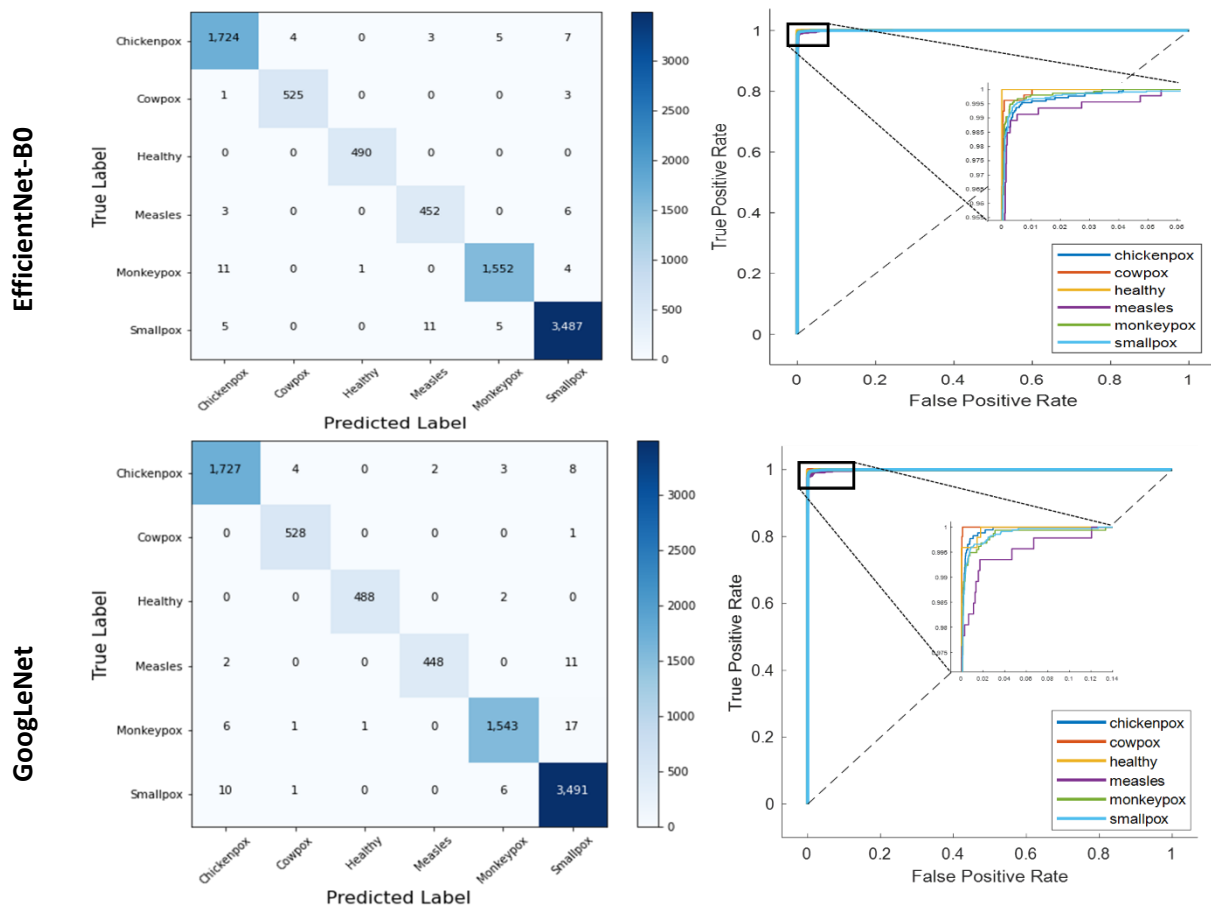


Figure 3. Confusion matrices and ROC curves of models for augmented data (a)

MobileNet V2

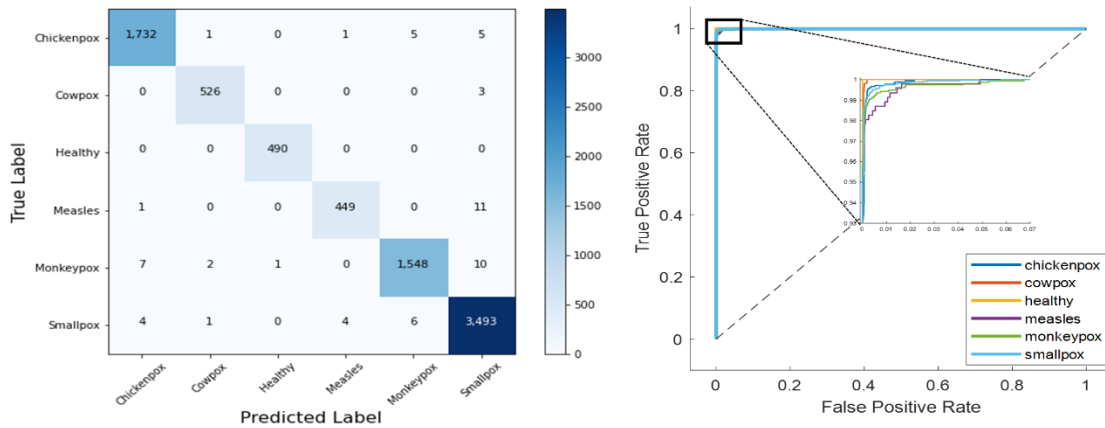
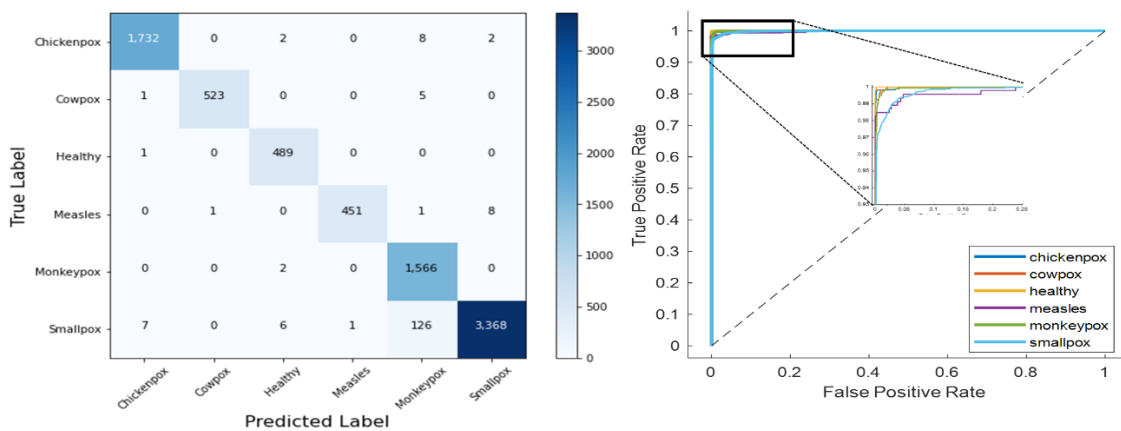


Figure 3. Confusion matrices and ROC curves of models for augmented data (a) (Continued)

VGG-16



VGG-19

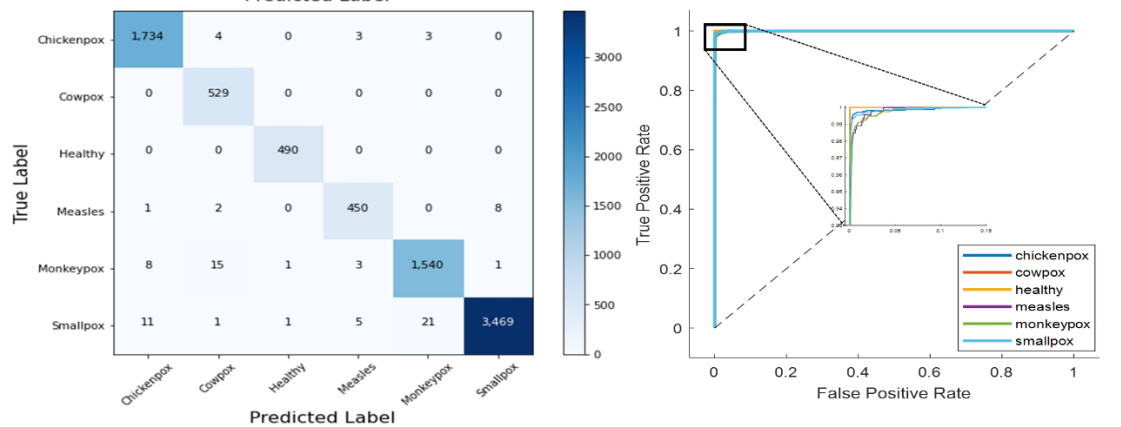


Figure 4. Confusion matrices and ROC curves of models for augmented data (b)

EfficientNet-B0

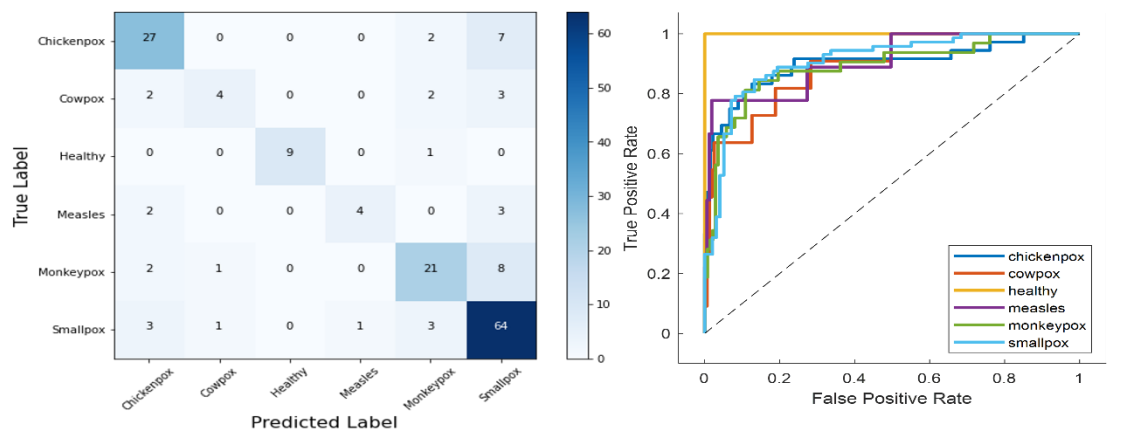


Figure 5. Confusion matrices and ROC curves of models for original data (a)

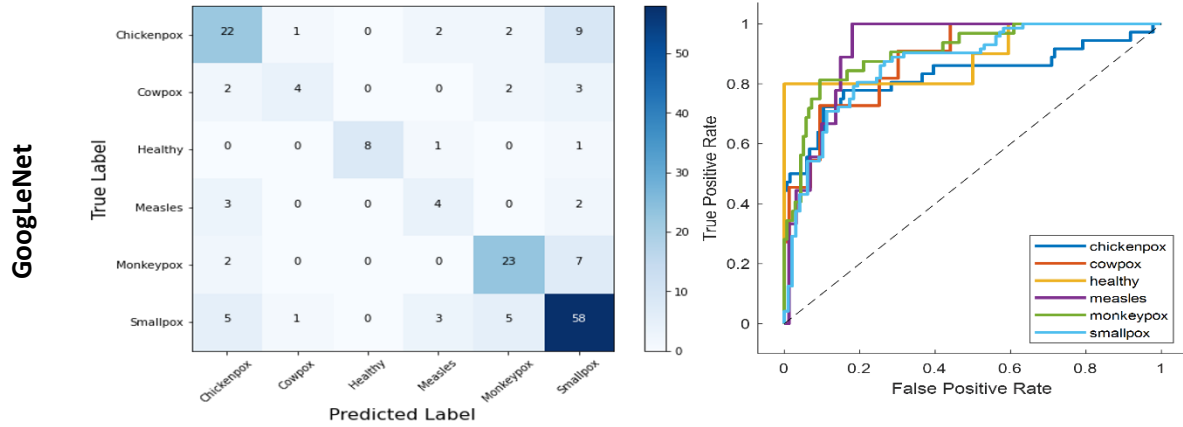


Figure 5. Confusion matrices and ROC curves of models for original data (a) (Continued)

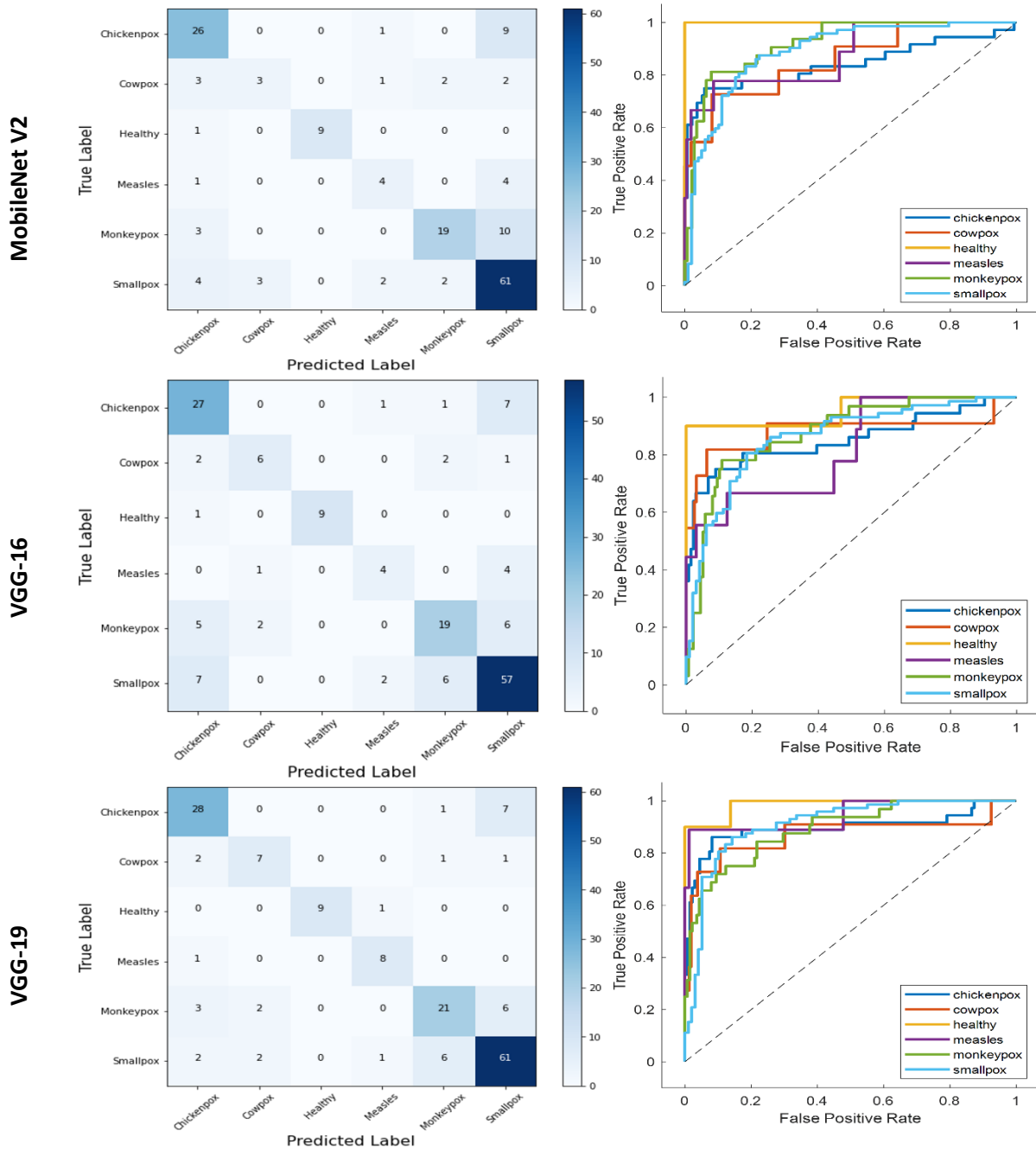


Figure 6. Confusion matrices and ROC curves of models for original data (b)

After obtaining the confusion matrices and ROC curves, the performance metrics mentioned in the previous section were calculated using the confusion matrices. Table 3 shows the results obtained from the augmented data and Table 4 shows the results obtained from the original data.

Table 3. Performance metrics for augmented data

| Model | Accuracy | Precision | Recall | F1 Score | AUC |
|-----------------|---------------|---------------|---------------|---------------|---------------|
| VGG-16 | 0.9794 | 0.9809 | 0.9861 | 0.9832 | 0.9995 |
| VGG-19 | 0.9894 | 0.9838 | 0.9902 | 0.9869 | 0.9998 |
| EfficientNet-B0 | 0.9917 | 0.9895 | 0.9909 | 0.9902 | 0.9998 |
| MobileNet V2 | 0.9925 | 0.9929 | 0.9907 | 0.9918 | 0.9999 |
| GoogLeNet | 0.991 | 0.9924 | 0.9892 | 0.9908 | 0.9998 |

As seen in Table 3, it is observed that the values obtained from the augmented data are higher. Looking at the values obtained, it is seen that MobileNet V2 network with 99.25% accuracy shows the highest performance. This is followed by EfficientNet-B0 and GoogLeNet. VGG-16 and VGG-19 were below 99% and achieved accuracies of 97.94% and 98.94% respectively.

Table 4. Performance metrics for original data

| Model | Accuracy | Precision | Recall | F1 Score | AUC |
|-----------------|---------------|---------------|---------------|--------------|---------------|
| VGG-16 | 0.7135 | 0.7147 | 0.6635 | 0.6824 | 0.8733 |
| VGG-19 | 0.7882 | 0.7919 | 0.7844 | 0.787 | 0.916 |
| EfficientNet-B0 | 0.7588 | 0.77823 | 0.6672 | 0.7072 | 0.9172 |
| MobileNet V2 | 0.7176 | 0.7033 | 0.6301 | 0.6561 | 0.8972 |
| GoogLeNet | 0.7 | 0.6929 | 0.6239 | 0.6485 | 0.8834 |

Table 4 presents the performance metrics derived from the original data. It is clear that the values in Table 4 are lower than the values in Table 3. Since the number of images in the original data is small, the CNN networks could not learn sufficiently, and therefore, the values obtained were lower. According to the table, VGG-19 had the best classification performance with 78.82% accuracy, and GoogLeNet had the lowest classification performance with 70% accuracy. Between these two models are EfficientNet-B0 (78.88%), MobileNet V2 (71.76%) and VGG-16 (71.35%), respectively.

CONCLUSION

As cases of monkeypox increase, the diagnosis and identification of the disease is becoming increasingly important. The fact that pox diseases show similar symptoms and the lesions on the body are similar to each other can negatively affect the diagnostic process. Therefore, researchers have been working on artificial intelligence-based computer-aided systems to help experts in the diagnosis process and to provide at least an idea during diagnosis. In this way, the diagnosis time is minimized, and diagnosis can be made more easily. Deep learning is at the forefront of AI-based computer-aided systems. CNN models, which are among the deep learning methods, have been very successful in making inferences from images. Therefore, in this study, monkeypox and other smallpox diseases were diagnosed using pretrained CNN models. GoogLeNet, EfficientNet-B0, MobileNet V2, VGG-16, and VGG-19 models were used as pre-trained CNN models. These models have a 224x224x3 input layer and an output layer with 1000 classes. Because six classes were used in the dataset, the output layers were revised and replaced with a 6-class layer. There were two different files in the dataset. One of these files contains the original data, whereas the other file contains augmented data. In this study, the data from both files were used separately for training and validation. As a result of the training and validation, Figures 3 and 4 show the confusion matrices and ROC curves obtained from the augmented data, whereas Figures 5 and 6 show the confusion matrices and ROC curves obtained from the original data. The confusion matrices were used to calculate the performance metrics needed to compare the

model performances. Tables 3 and 4 show the performance metrics of all the models. According to these values, MobileNet V2 with augmented data achieved the highest classification accuracy of 99.25% and VGG-19 with the original data achieved the highest classification accuracy of 78.82%.

Conflict of Interest

The article authors declare that there is no conflict of interest between them.

Author's Contributions

The authors declare that they have contributed equally to the article.

KAYNAKLAR

- Ahsan, M. M., Uddin, M. R., Farjana, M., Sakib, A. N., Momin, K. al, & Luna, S. A. (2022). *Image Data collection and implementation of deep learning-based model in detecting Monkeypox disease using modified VGG16*. <https://doi.org/10.48550/arxiv.2206.01862>
- Alenezi, F., Armghan, A., & Polat, K. (2023). Wavelet transform based deep residual neural network and ReLU based Extreme Learning Machine for skin lesion classification. *Expert Systems with Applications*, 213, 119064. <https://doi.org/10.1016/J.ESWA.2022.119064>
- Ali, S. N., Ahmed, Md. T., Paul, J., Jahan, T., Sani, S. M. S., Noor, N., & Hasan, T. (2022). *Monkeypox Skin Lesion Detection Using Deep Learning Models: A Feasibility Study*. <https://doi.org/10.48550/arxiv.2207.03342>
- Aljaddouh, B., & Malathi, D. (2022). Trends of using machine learning for detection and classification of respiratory diseases: Investigation and analysis. *Materials Today: Proceedings*, 62, 4651–4658. <https://doi.org/10.1016/J.MATPR.2022.03.120>
- Bayat, S., & Işık, G. (2022). Aras Kuş Türlerinin Ses Özellikleri Bakımından Derin Öğrenme Yöntemleriyle Tanınması. *Journal of the Institute of Science and Technology*, 12(3), 1250–1263. <https://doi.org/10.21597/JIST.1124674>
- Bhatt, H., Shah, V., Shah, K., Shah, R., & Shah, M. (2022). State-of-the-art machine learning techniques for melanoma skin cancer detection and classification: a comprehensive review. *Intelligent Medicine*. <https://doi.org/10.1016/J.IMED.2022.08.004>
- Bhattacharjee, S., Saha, B., Bhattacharyya, P., & Saha, S. (2022). Classification of obstructive and non-obstructive pulmonary diseases on the basis of spirometry using machine learning techniques. *Journal of Computational Science*, 63, 101768. <https://doi.org/10.1016/J.JOCS.2022.101768>
- Bunge, E. M., Hoet, B., Chen, L., Lienert, F., Weidenthaler, H., Baer, L. R., & Steffen, R. (2022). The changing epidemiology of human monkeypox—A potential threat? A systematic review. *PLOS Neglected Tropical Diseases*, 16(2), e0010141. <https://doi.org/10.1371/JOURNAL.PNTD.0010141>
- CDC. (n.d.). *2022 Outbreak Cases and Data | Monkeypox | Poxvirus | CDC*. Retrieved October 30, 2022, from <https://www.cdc.gov/poxvirus/monkeypox/response/2022/index.html>
- Elashiri, M. A., Rajesh, A., Nath Pandey, S., Kumar Shukla, S., Urooj, S., & Lay-Ekuakille, A. (2022). Ensemble of weighted deep concatenated features for the skin disease classification model using modified long short term memory. *Biomedical Signal Processing and Control*, 76, 103729. <https://doi.org/10.1016/J.BSPC.2022.103729>
- Ferreira, M. I. A. S. N., Barbieri, F. A., Moreno, V. C., Penedo, T., & Tavares, J. M. R. S. (2022). Machine learning models for Parkinson's disease detection and stage classification based on spatial-temporal gait parameters. *Gait & Posture*, 98, 49–55. <https://doi.org/10.1016/J.GAITPOST.2022.08.014>

- Hu, Y., Wen, C., Cao, G., Wang, J., & Feng, Y. (2022). Brain network connectivity feature extraction using deep learning for Alzheimer's disease classification. *Neuroscience Letters*, 782, 136673. <https://doi.org/10.1016/J.NEULET.2022.136673>
- Ibrahim, D. M., Elshennawy, N. M., & Sarhan, A. M. (2021). Deep-chest: Multi-classification deep learning model for diagnosing COVID-19, pneumonia, and lung cancer chest diseases. *Computers in Biology and Medicine*, 132, 104348. <https://doi.org/10.1016/J.COMPBIOMED.2021.104348>
- Inik, Ö., & Turan, B. (2018). *Classification of Different Age Groups of People by Using Deep Learning*. <https://www.researchgate.net/publication/333045149>
- Inik, O., Uyar, K., & Ülker, E. (2019). *Gender Classification with A Novel Convolutional Neural Network (CNN) Model and Comparison with other Machine Learning and Deep Learning CNN Models*. <https://www.researchgate.net/publication/330279739>
- Islam, T., Hussain, M. A., Uddin, F., Chowdhury, H., & Islam, B. M. R. (2022). Can Artificial Intelligence Detect Monkeypox from Digital Skin Images? *BioRxiv*, 2022.08.08.503193. <https://doi.org/10.1101/2022.08.08.503193>
- Jia, Z., & Chen, D. (2020). Brain Tumor Identification and Classification of MRI images using deep learning techniques. *IEEE Access*, 1–1. <https://doi.org/10.1109/ACCESS.2020.3016319>
- Krizhevsky, A., & Inc, G. (2014). *One weird trick for parallelizing convolutional neural networks*. <https://doi.org/10.48550/arxiv.1404.5997>
- Li, Y., Luo, J. hao, Dai, Q. yun, Eshraghian, J. K., Ling, B. W. K., Zheng, C. yan, & Wang, X. li. (2023). A deep learning approach to cardiovascular disease classification using empirical mode decomposition for ECG feature extraction. *Biomedical Signal Processing and Control*, 79, 104188. <https://doi.org/10.1016/J.BSPC.2022.104188>
- Memariani, M., & Memariani, H. (2022). Multinational monkeypox outbreak: what do we know and what should we do? *Irish Journal of Medical Science (1971 -)* 2022, 1–2. <https://doi.org/10.1007/S11845-022-03052-4>
- Monisha, M., Suresh, A., & Rashmi, M. R. (2018). Artificial Intelligence Based Skin Classification Using GMM. *Journal of Medical Systems*, 43(1), 1–8. <https://doi.org/10.1007/S10916-018-1112-5/FIGURES/12>
- WHO. (n.d.). *Monkeypox*. Retrieved October 30, 2022, from <https://www.who.int/news-room/fact-sheets/detail/monkeypox>
- monkeypox 2022 remastered | Kaggle*. (n.d.). Retrieved November 5, 2022, from <https://www.kaggle.com/datasets/maxmelichov/monkeypox-2022-remastered>
- Muñoz-Saavedra, L., Escobar-Linero, E., Civit-Masot, J., Luna-Perejón, F., Civit, A., & Domínguez-Morales, M. (2022). Monkeypox Diagnostic-Aid System with Skin Images Using Convolutional Neural Networks. *SSRN Electronic Journal*. <https://doi.org/10.2139/SSRN.4186534>
- Nguyen, D., Nguyen, H., Ong, H., Le, H., Ha, H., Duc, N. T., & Ngo, H. T. (2022). Ensemble learning using traditional machine learning and deep neural network for diagnosis of Alzheimer's disease. *IBRO Neuroscience Reports*, 13, 255–263. <https://doi.org/10.1016/J.IBNEUR.2022.08.010>
- Pacal, İ. (2022). Deep Learning Approaches for Classification of Breast Cancer in Ultrasound (US) Images. *Journal of the Institute of Science and Technology*, 12(4), 1917–1927. <https://doi.org/10.21597/JIST.1183679>
- Pacal, I., & Karaboga, D. (2021). A robust real-time deep learning based automatic polyp detection system. *Computers in Biology and Medicine*, 134, 104519. <https://doi.org/10.1016/J.COMPBIOMED.2021.104519>
- Pacal, I., Karaboga, D., Basturk, A., Akay, B., & Nalbantoglu, U. (2020). A comprehensive review of deep learning in colon cancer. *Computers in Biology and Medicine*, 126, 104003. <https://doi.org/10.1016/J.COMPBIOMED.2020.104003>

- Parker, S., & Buller, R. M. (2013). A review of experimental and natural infections of animals with monkeypox virus between 1958 and 2012. *Http://Dx.Doi.Org/10.2217/Fvl.12.130*, 8(2), 129–157. <https://doi.org/10.2217/FVL.12.130>
- Qian, S., Ren, K., Zhang, W., & Ning, H. (2022). Skin lesion classification using CNNs with grouping of multi-scale attention and class-specific loss weighting. *Computer Methods and Programs in Biomedicine*, 226, 107166. <https://doi.org/10.1016/J.CMPB.2022.107166>
- Rezaee, K., Savarkar, S., Yu, X., & Zhang, J. (2022). A hybrid deep transfer learning-based approach for Parkinson's disease classification in surface electromyography signals. *Biomedical Signal Processing and Control*, 71, 103161. <https://doi.org/10.1016/J.BSPC.2021.103161>
- Sandler, M., Howard, A., Zhu, M., Zhmoginov, A., & Chen, L. C. (2018). MobileNetV2: Inverted Residuals and Linear Bottlenecks. *Proceedings of the IEEE Computer Society Conference on Computer Vision and Pattern Recognition*, 4510–4520. <https://doi.org/10.48550/arxiv.1801.04381>
- Shinde, A. S., Mahendra, B., Nejakar, S., Herur, S. M., & Bhat, N. (2022). Performance analysis of machine learning algorithm of detection and classification of brain tumor using computer vision. *Advances in Engineering Software*, 173, 103221. <https://doi.org/10.1016/J.ADVENGSOFT.2022.103221>
- Simonyan, K., & Zisserman, A. (2014). Very Deep Convolutional Networks for Large-Scale Image Recognition. *3rd International Conference on Learning Representations, ICLR 2015 - Conference Track Proceedings*. <https://doi.org/10.48550/arxiv.1409.1556>
- Swathy, M., & Saruladha, K. (2022). A comparative study of classification and prediction of Cardio-Vascular Diseases (CVD) using Machine Learning and Deep Learning techniques. *ICT Express*, 8(1), 109–116. <https://doi.org/10.1016/J.ICTE.2021.08.021>
- Talukder, M. A., Islam, M. M., Uddin, M. A., Akhter, A., Hasan, K. F., & Moni, M. A. (2022). Machine learning-based lung and colon cancer detection using deep feature extraction and ensemble learning. *Expert Systems with Applications*, 205, 117695. <https://doi.org/10.1016/J.ESWA.2022.117695>
- Tan, M., & Le, Q. v. (2019). EfficientNet: Rethinking Model Scaling for Convolutional Neural Networks. *36th International Conference on Machine Learning, ICML 2019, 2019-June*, 10691–10700. <https://doi.org/10.48550/arxiv.1905.11946>
- Vankdothu, R., & Hameed, M. A. (2022). Brain tumor segmentation of MR images using SVM and fuzzy classifier in machine learning. *Measurement: Sensors*, 24, 100440. <https://doi.org/10.1016/J.MEASEN.2022.100440>
- Vuidel, A., Cousin, L., Weykopf, B., Haupt, S., Hanifehlou, Z., Wiest-Daesslé, N., Segschneider, M., Lee, J., Kwon, Y.-J., Peitz, M., Ogier, A., Brino, L., Brüstle, O., Sommer, P., & Wilbertz, J. H. (2022). High-content phenotyping of Parkinson's disease patient stem cell-derived midbrain dopaminergic neurons using machine learning classification. *Stem Cell Reports*, 17(10), 2349–2364. <https://doi.org/10.1016/J.STEMCR.2022.09.001>
- Wei, Z., Li, Q., & Song, H. (2022). Dual attention based network for skin lesion classification with auxiliary learning. *Biomedical Signal Processing and Control*, 74, 103549. <https://doi.org/10.1016/J.BSPC.2022.103549>
- Xin, C., Liu, Z., Zhao, K., Miao, L., Ma, Y., Zhu, X., Zhou, Q., Wang, S., Li, L., Yang, F., Xu, S., & Chen, H. (2022). An improved transformer network for skin cancer classification. *Computers in Biology and Medicine*, 149, 105939. <https://doi.org/10.1016/J.COMPBIOMED.2022.105939>
- Zhou, J., Wu, Z., Jiang, Z., Huang, K., Guo, K., & Zhao, S. (2022). Background selection schema on deep learning-based classification of dermatological disease. *Computers in Biology and Medicine*, 149, 105966. <https://doi.org/10.1016/J.COMPBIOMED.2022.105966>